On the climatic influence of CO_2 forcing in the Pliocene

Lauren E. Burton[1], Alan M. Haywood[1], Julia C. Tindall[1], Aisling M. Dolan[1], Daniel J. Hill[1], Ayako Abe-Ouchi[2], Wing-Le Chan[2], Deepak Chandan[3], Ran Feng[4], Stephen J. Hunter[1], Xiangyu Li[5], W. Richard Peltier[3], Ning Tan[6], Christian Stepanek[7], Zhongshi Zhang[8]

[1]School of Earth and Environment, University of Leeds, Woodhouse Lane, Leeds, West Yorkshire, LS2 9JT, UK
[2]Atmosphere and Ocean Research Institute, The University of Tokyo, Kashiwa, 277-8564, Japan
[3]Department of Physics, University of Toronto, Toronto, M5S 1A7, Canada
[4]Department of Geosciences, College of Liberal Arts and Sciences, University of Connecticut, Storrs, CT 06033, USA
[5]Department of Atmospheric Science, School of Environmental Studies, China University of Geoscience, Wuhan, 430074, China
[6]Key Laboratory of Cenozoic Geology and Environment, Institute of Geology and Geophysics, Chinese Academy of Sciences, Beijing, 100029, China
[7]Alfred-Wegener-Institut – Helmholtz-Zentrum für Polar and Meeresforschung (AWI), Bremerhaven, 27570, Germany
[8]NORCE Norwegian Research Centre, Bjerknes Centre for Climate Research, 5007 Bergen, Norway

Correspondence to: Lauren E. Burton (eeleb@leeds.ac.uk)

Abstract. Understanding the dominant climate forcings in the Pliocene is crucial to assessing the usefulness of the Pliocene as an analogue for our warmer future. Here we implement a novel, yet simple linear factorisation method to assess the relative influence of CO_2 forcing in seven models of the Pliocene Model Intercomparison Project Phase 2 (PlioMIP2) ensemble. Outputs are termed "FCO_2" and show the fraction of Pliocene climate change driven by CO_2.

The accuracy of the FCO_2 method is first assessed through comparison to an energy balance analysis previously used to assess drivers of surface air temperature in the PlioMIP1 ensemble. After this assessment, the FCO_2 method is applied to achieve an understanding of the drivers of Pliocene sea surface temperature and precipitation for the first time.

CO_2 is found to be the most important forcing in the ensemble for Pliocene surface air temperature (global mean $FCO_2 = 0.56$), sea surface temperature (global mean $FCO_2 = 0.56$) and precipitation (global mean $FCO_2 = 0.51$). The range between individual models is found to be consistent between these three climate variables, and the models generally show good agreement on the sign of the most important forcing.

Our results provide the most spatially complete view of the drivers of Pliocene climate to date, and have implications for both data-model comparison and the use of the Pliocene as an analogue for the future. That CO_2 is found to be the most important forcing reinforces that the Pliocene is a good palaeoclimate analogue, but the significant effect of non-CO_2 forcing at regional scale (e.g. orography and ice sheet forcing at high-latitudes) reminds us that it is not perfect, and these additional influencing factors must not be overlooked. This comparison is further complicated when considering the Pliocene as a state in quasi-equilibrium with CO_2 forcing compared to the transient warming being experienced at present.

1 Introduction

1.1 Pliocene climate modelling and PlioMIP

The mid-Piacenzian Warm Period (mPWP, previously referred to as the mid-Pliocene Warm Period), 3.264-3.025 Ma, is of great interest to the palaeoclimate community as a potential analogue for future climate change (Haywood et al., 2011a; Burke et al., 2018). It was the most recent period of sustained warmth above pre-industrial (PI) temperatures, is recent enough to have a continental configuration similar to modern and has similar-to-modern atmospheric CO_2 concentration at ~400 ppm (Pagani et al., 2010; Seki et al., 2010; Bartoli et al., 2011; de la Vega et al., 2020).

Given its potential as a palaeoclimate analogue, the study of the Pliocene has been central to palaeoclimate modelling efforts over the past three decades. In 2008, the Pliocene Model Intercomparison Project (PlioMIP) was introduced as a working group of the Palaeooclimate Model Intercomparison Project (PMIP) to further our understanding of the Pliocene climate and, in turn, its accuracy and usefulness as a palaeoclimate analogue.

PlioMIP1 focused on a climatically distinct 'time slab' spanning 3.29-2.97 Ma with temperatures generally warmer than present (Dowsett et al., 1999; 2007). PlioMIP1 comprised two experiments: seven modelling groups completed Experiment 1 with atmosphere-only climate models (Haywood et al., 2010) and eight modelling groups completed Experiment 2 with fully coupled atmosphere-ocean climate models (Haywood et al., 2011b). The large-scale feature results from PlioMIP1 were presented in Haywood et al. (2013). The ensemble showed a global mean surface air temperature (SAT) Pliocene-PI anomaly of 1.97-2.80°C and 1.84-3.60°C in Experiment 1 and Experiment 2 respectively, associated with an increase in precipitation of 0.04-0.11 mm day^{-1} and 0.09-0.18 mm day^{-1}. Equilibrium climate sensitivity (ECS) varied between models, with an ensemble mean of 3.36°C and an Earth System Sensitivity (ESS) to ECS ratio of 1.5.

The second phase, PlioMIP2, saw the implementation of new boundary conditions in response to data-model comparison (DMC) studies of PlioMIP1 and the move from a time slab approach to a time slice focusing on a specific marine isotope stage within the mPWP with similar-to-modern orbital forcing, MIS KM5c, at 3.205 Ma. From here when we refer to the Pliocene, we are specifically referring to the MIS KM5c time slice. PlioMIP2 also saw the introduction of forcing factorisation experiments (Sect. 1.2), which allowed the influence of different climate forcings to be assessed, as well as an explicit "Pliocene4Future" element which enabled results to be directly relevant to discussions on climate sensitivity and the Pliocene as a palaeoclimate analogue (Haywood et al., 2016). Fourteen model groups contributed to PlioMIP2, including seven that contributed to PlioMIP1 (CCSM4, COSMOS, HadCM3, IPSLCM5A, MIROC4m, MRI-CGCM 2.3 and NorESM-L).

The large-scale feature results from PlioMIP2 were presented in Haywood et al. (2020). Global mean SAT was higher than that found in PlioMIP1, with an ensemble mean of 3.2°C warmer than the PI (range 1.7-5.2°C), partly due to the addition of models more sensitive to the Pliocene CO_2 forcing; the ensemble mean ECS was 3.7°C with an ESS to ECS ratio of 1.67. The increase in precipitation was also greater than seen in PlioMIP1, ranging from 0.07-0.37 mm day^{-1}.

The anomalies seen in PlioMIP2 are comparable to some of the Shared Socioeconomic Pathways (SSPs) shown in the Sixth Assessment Report of the Intergovernmental Panel on Climate Change (IPCC AR6; Fig. 1), reinforcing the potential to use

the Pliocene as a palaeoclimate analogue. The magnitude of global mean warming relative to the PI is comparable between the Pliocene (3.2°C; Haywood et al., 2020) and end of the century (2081-2100) estimates for SSP2-4.5 (2.7°C) and SSP3-7.0 (3.6°C; Lee et al., 2021), though the latter may look even more comparable to the Eocene (Burke et al., 2018; Lee et al., 2021).

70   There are also comparable spatial patterns of climate anomalies between end of the century and PlioMIP2 in the form of polar amplification and the land warming more than the ocean (Fig. 1a, b, c). The differences in polar amplification, and precipitation over Africa and the Middle East, can largely be explained by the differences in other boundary conditions, particularly ice sheet volume and extent and the impact this has on atmospheric circulation (e.g. Sun et al., 2013; Corvec and Fletcher, 2017).
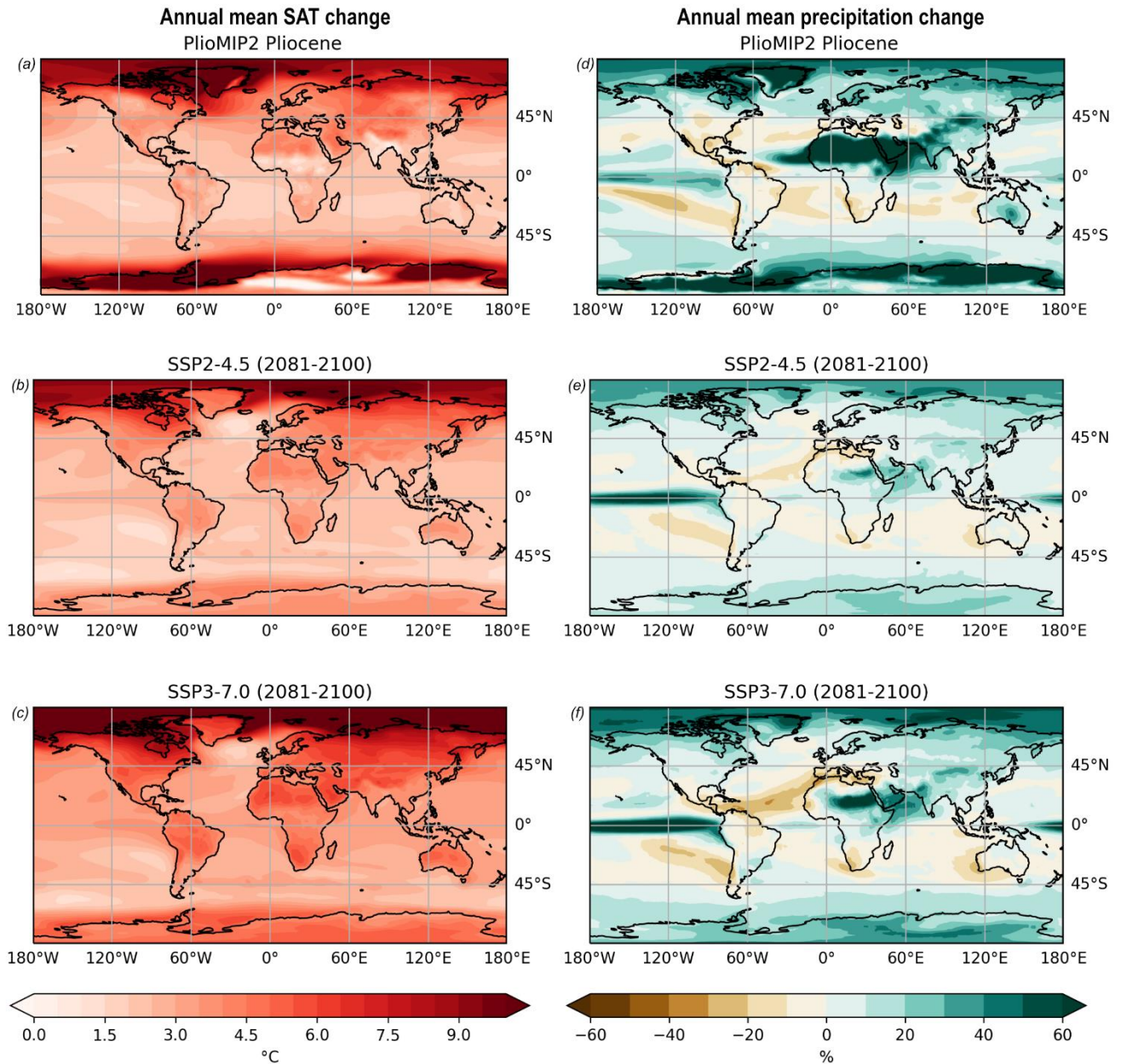
Figure 1: PlioMIP2 ensemble MIS KM5c SAT (a) and precipitation (d) anomalies relative to the PI compared to equivalent CMIP6 anomalies for 2081-2100 under SSP2-4.5 (c, d) and SSP3-7.0 (e, f). The PlioMIP2 ensemble includes all 16 models in Haywood et al. (2020) plus HadGEM3 (Williams et al., 2021). The CMIP6 data is from the IPCC WGI Interactive Atlas (Gutiérrez et al., 2021). CMIP6 SAT anomalies (c, d) are relative to 1850-1900, and precipitation anomalies (e, f) to the standard CMIP6 base period (1995-2014). Note that the models included in PlioMIP2 are not all included in CMIP6.

From the water cycle projections in the IPCC AR6 (Table 8.1 in Douville et al., 2021), it is clear that the global mean percentage change in precipitation is also comparable between 2081-2100 under SSP2-4.5 (4.0%) and SSP3-7.0 (5.1%) relative to the

CMIP6 base period (1995-2014) and the Pliocene (7%; Haywood et al., 2020). Similar spatial features include the wetting of the Sahara and polar regions, and drying of the Caribbean, off the western coast of South America (Fig. 1d, e, f).

However, caution must be applied when referencing the Pliocene as a palaeoclimate analogue given the importance of –
85 continually changing – anthropogenic greenhouse gas forcing in present day.

Here, we begin to assess the role of CO_2 forcing in the Pliocene compared to other drivers of climate and changes in boundary conditions. The non-CO_2 forcing we refer to includes changes to ice sheets and 'orography', the latter of which also includes changes to prescribed vegetation, bathymetry, land-sea mask, soils and lakes per the experimental design of PlioMIP2 (Haywood et al., 2016).

90 **1.2. Drivers of Pliocene climate**

Though there are similarities in large-scale climate features between the Pliocene and end-of-century projections in AR6, the similarity in the causes and drivers of some of these features is yet to be fully assessed.

Previous studies on the drivers of Pliocene temperature change have used energy balance analyses. These are commonly applied in palaeoclimate studies to understand changes in temperature by separating out individual forcing components (e.g.
95 Lunt et al., 2012; Hill et al., 2014 and references therein).

Lunt et al. (2012) combined a novel factorisation methodology with energy balance analysis to assess the causes of Pliocene warmth in HadCM3 using the PRISM2 boundary conditions (Dowsett et al., 1999). CO_2 was found to cause 36-61% of Pliocene warmth, orography 0-26%, ice sheets 9-13% and vegetation 21-27%. These drivers were found to have spatial variation in importance, with changes in orography and ice sheets particularly important in driving polar amplification in the
100 northern high-latitudes, and orography particularly important in the southern high-latitudes. The energy balance analysis also highlighted how surface albedo changes and direct CO_2 forcing contributed more than cloud feedbacks, with surface albedo changes dominating at mid- and high-latitudes and CO_2 forcing at low latitudes.

Hill et al. (2014) developed the methodology of Lunt et al. (2012) and conducted the first multi-model energy balance analysis using the eight models included in PlioMIP1 Experiment 2, forced with the PRISM3 boundary conditions. Greenhouse gas
105 emissivity was found to be the dominant cause of warming in the tropics. There were large uncertainties between models in the high latitudes but all energy balance components were important, and clear sky albedo was the dominant driver of polar amplification through reductions in ice sheets, sea ice and snow cover and changes to vegetation. The relative influence of the energy balance components was more uncertain in the northern mid-latitudes, particularly in the North Atlantic and Kuroshio Current regions, where warming was also simulated differently between models (Haywood et al., 2013).
110 Developing from PlioMIP1, forcing factorisation experiments were included in PlioMIP2 to enable the explicit assessment of forcing components (Haywood et al., 2016). These experiments included Pliocene simulations with PI ice configuration (experiment Eo^{400}) and PI orography configuration (experiment Ei^{400}), as well as a PI simulation with Pliocene-level CO_2 concentration (experiment E^{400}); the PlioMIP2 experimental design and naming conventions were shown in Haywood et al.

(2016). These forcing factorisation experiments were in Tier 2 of the experimental design, meaning they were optional and completed by a smaller number of model groups.

The impact of various mechanisms on Pliocene climate has been studied using energy balance analysis in individual PlioMIP2 models. Using the PlioMIP2 forcing factorisation experiments and methodology proposed in Haywood et al. (2016), Chandan and Peltier (2018) assessed the mechanisms of Pliocene climate in the CCSM4-UoT model. They found that around 1.67°C (45%) of warming was attributable to CO_2 forcing, 1.54°C (42%) to changes in orography and 0.47°C (13%) to a reduction in ice sheets. Using the same factorisation methodology for the COSMOS model, Stepanek et al. (2020) found that 2.23°C (~66%) of warming was attributable to CO_2 forcing, 0.91°C (~25%) to orography and 0.38°C (~13%) to changes in the ice sheets.

An updated methodology of Lunt et al. (2012) and Hill et al. (2014) is used to explore drivers of northern high-latitude warmth in the CCSM4 model in Feng et al. (2017). Changes to regional topography, Arctic sea ice and the Greenland ice sheet, and the North Atlantic meridional overturning circulation were found to explain the amplification of SAT in the northern high-latitudes. Greenhouse gas emissivity was also found to be important, particularly with the subsequent positive feedbacks which have a more distributed effect. This updated methodology is also used in Feng et al. (2019) where it is demonstrated that a seasonally sea ice-free Pliocene Arctic Ocean can be simulated in CESM1.2 by including aerosol-cloud interactions and excluding industrial pollutants.

To date, there has been no systematic study comparing multiple models in the PlioMIP2 ensemble to spatially quantify the importance of different climate forcings, nor have climate variables other than SAT been previously assessed in multiple models in a single study. Here, we present the relative spatial influence of CO_2 forcing for SAT across multiple PlioMIP2 models and, for the first time, sea surface temperature (SST) and precipitation. We employ the forcing factorisation experiments of PlioMIP2 and a novel, simple linear factorisation method with outputs we term "FCO_2".

2. Methods

2.1. Model boundary conditions

Standardised boundary conditions are used by all model groups for the core Pliocene control experiment in PlioMIP2, derived from the U.S. Geological Survey PRISM4 reconstruction (Dowsett et al., 2016) and implemented as described in Haywood et al. (2016). These boundary conditions include spatially-complete gridded datasets at 1° x 1° of latitude-longitude for land-sea distribution, topography and bathymetry, vegetation, soil, lakes and land ice cover; all models analysed here use the "enhanced" version of the boundary conditions, meaning they include all reconstructed changes to the land-sea mask and ocean bathymetry (Haywood et al., 2020).

The configuration of the Greenland ice sheet in PRISM4 is based upon the results from the Pliocene Ice Sheet Modelling Intercomparison Project (PLISMIP): it is confined to high elevations in the Eastern Greenland Mountains and covers an area around 25% of the modern ice sheet (Dolan et al., 2015; Koenig et al., 2015). Ice coverage over Antarctica has been debated (see Levy et al., 2022) but the PRISM3 Antarctic ice configuration – in which there is a reduction in the ice margins in the

Wilkes and Aurora basins in eastern Antarctica, and western Antarctica is largely ice free (Dowsett et al., 2010) – is supported and so retained in the PRISM4 reconstruction (Dowsett et al., 2016). Later modelling studies further support the potential for ice retreat in similar areas in Antarctica under the warmer temperatures of the Pliocene (e.g. DeConto and Pollard, 2016). The palaeogeography is broadly similar to modern except for the closure of the Bering Strait and Canadian Arctic Archipelago;

150 changes in the Torres Strait, Java Sea, South China Sea, Kara Strait; and a West Antarctic Seaway (Haywood et al., 2016). PRISM4 also includes dynamic topography and glacial isostatic adjustment for the first time to inform the representation of local sea level (Dowsett et al., 2016).

Atmospheric CO_2 concentration is set to 400 ppm and, in the absence of proxy data, all other trace gases are set to be identical to the concentrations in the PI control experiment for each individual model group (Haywood et al., 2016).

155 **2.2. Participating models**

Seven of the 17 models of the PlioMIP2 ensemble are included in this study as they conducted the necessary experiments to apply our novel FCO_2 method: Eoi^{400}, E^{400} and E^{280} (see Sect. 2.3). This subgroup is also found to be representative of the wider PlioMIP2 ensemble in terms of modelled ECS, ESS and global mean Eoi^{400}-E^{280} SAT anomaly (Table 1).

Parameter	PlioMIP2	This ensemble
ECS (°C)	3.7	3.8
ESS (°C)	6.2	6.1
ESS to ECS ratio	1.7	1.7
Eoi^{400}-E^{280} SAT anomaly (°C)	3.2	3.2

Table 1: A comparison of climate parameters between the PlioMIP2 ensemble and the subgroup of PlioMIP2 models used here.

160 The models are of varying ages and resolutions. Summary details relevant to PlioMIP2 are shown in Haywood et al. (2020) and in individual model papers for the PlioMIP2 experiments which are cited in Table 2.

Model	Vintage	Sponsor(s), country	Eoi^{400} boundary conditions and experiment citation	Climate sensitivity (ECS; °C) and citation
CCSM4-UoT	2011	University of Toronto, Canada	Enhanced with fixed vegetation (Chandan and Peltier, 2017; 2018)	3.2 (Peltier and Vettoretti, 2014; Chandan and Peltier, 2018)
CESM2	2020	National Center for Atmospheric Research, USA	Enhanced with fixed vegetation (Feng et al., 2020)	5.3 (Gettelman et al., 2019)
COSMOS	2009	Alfred Wegener Institute, Germany	Enhanced with dynamic vegetation (Stepanek et al., 2020)	4.7 (Stepanek et al., 2020)
HadCM3	1997	University of Leeds, UK	Enhanced with fixed vegetation (Hunter et al., 2019)	3.5 (Hunter et al., 2019)
IPSLCM5A2	2017	LSCE, France	Enhanced with fixed vegetation (Tan et al., 2020)	3.6 (reported in Haywood et al., 2020)

MIROC4m	2004	Center for Climate Research (Uni. Tokyo, National Inst. For Env. Studies, Frontier Research Center for Global Change, JAMSTEC), Japan	Enhanced with fixed vegetation (Chan and Abe-Ouchi, 2020)	3.9 (Chan and Abe-Ouchi, 2020)
NorESM1-F	2017	NORCE Norwegian Research Centre, Bjerknes Centre for Climate Research, Bergen, Norway	Enhanced with fixed vegetation (Li et al., 2020)	2.3 (Guo et al., 2019)

Table 2: Details of the climate models used in the FCO$_2$ analysis (adapted from Haywood et al., 2020).

2.3. FCO$_2$ method

Taking advantage of the forcing factorisation experiments included in the PlioMIP2 experimental design, here we propose a
165 novel simple linear factorisation method to assess the influence of CO$_2$ forcing with outputs we term "FCO$_2$". We apply the
FCO$_2$ method to all seven models for SAT and precipitation, and to six models for SST; IPSLCM5A2 is excluded for analysis
of the latter as only 10 model years of data were available.

The method uses three PlioMIP2 experiments: the two core experiments (E^{280} and Eoi^{400}) and one Tier 2 experiment (E^{400}; Table 3). Core experiments were completed by all PlioMIP2 modelling groups and Tier 2 experiments were submitted by a
170 smaller number of modelling groups. The seven models included here were the only ones to have reported E^{400} results by the time of compiling this study.

ID	Description	Land-sea mask	Topography	Ice	Vegetation	CO$_2$ (ppm)	Status
Eoi^{400}	Pliocene control experiment	Pliocene - Modern	Pliocene	Pliocene	Dynamic	400	Core
E^{280}	PI control	Modern	Modern	Modern	Dynamic	280	Core
E^{400}	PI experiment with CO$_2$ concentration of 400 ppm	Modern	Modern	Modern	Dynamic	400	Tier 2 – Pliocene4Future and Pliocene4Pliocene

Table 3: Details of the PlioMIP2 experiments included in the FCO$_2$ analysis (adapted from Haywood et al., 2016). Note that dynamic vegetation was optional in the experimental design: only COSMOS ran with dynamic vegetation and all other models ran with the prescribed vegetation of Salzmann et al. (2008). As COSMOS ran with dynamic vegetation, some vegetation feedback in this model
175 **will be included in the E^{400}-E^{280} anomaly.**

We define FCO$_2$ as an approximation of the relative influence of CO$_2$ calculated by:

$$FCO_2 = \frac{(E^{400}-E^{280})}{(Eoi^{400}-E^{280})}$$ (1)

where E^{400}-E^{280} represents the change in climate caused by the change in CO$_2$ concentration from 280 ppm to 400 ppm alone, and Eoi^{400}-E^{280} represents the change in climate as a result of implementing the full Pliocene boundary conditions.

180 FCO_2 is therefore a fractional quantity where a value of 1.0 denotes that the signal of change is wholly dominated by CO_2 forcing, and a value of 0.0 denotes the contrasting case where the climate signal wholly is dominated by non-CO_2 forcing. Here, non-CO_2 forcing is defined as changes to ice sheets and orography, the latter of which includes changes to prescribed vegetation, bathymetry, land-sea mask, soils and lakes per the PlioMIP2 experimental design (Haywood et al., 2016). Our full interpretation of the range of FCO_2 values is shown in Table 4.

FCO_2 value	Interpretation relative to signal of change
>1.0	Wholly dominated by CO_2 forcing with some non-CO_2 forcing acting in the opposite direction to the overall climate signal
0.8-1.0	Highly dominated by CO_2 forcing
0.6-0.8	Dominated by CO_2 forcing
0.5-0.6	Mixed forcing but CO_2 forcing dominant
0.4-0.5	Mixed forcing but non-CO_2 forcing dominant
0.2-0.4	Dominated by non-CO_2 forcing
0.0-0.2	Highly dominated by non-CO_2 forcing
<0.0	Wholly dominated by non-CO_2 forcing with some CO_2 forcing acting in the opposite direction to the overall climate signal

185 **Table 4: Interpretation of FCO_2 values.**

FCO_2 values are not limited between 0.0 and 1.0. FCO_2 values above 1.0 represent a climate that is wholly dominated by CO_2 forcing where non-CO_2 forcing creates an opposing climatic effect. Similarly, FCO_2 values below 0.0 represent a climate that is wholly dominated by non-CO_2 forcing where CO_2 forcing creates an opposing climatic effect.

This becomes clear if one considers FCO_2 in the case of SAT and SST. The Pliocene climate is characterised as having elevated
190 temperature and CO_2 concentration compared to the PI (e.g. Dowsett et al., 2016; Haywood et al., 2020) so, given that the predominant effect of CO_2 forcing is warming, an FCO_2 value below 0.0 is rare. An exception is provided by higher-order effects where CO_2 leads to a cooling (see Sherwood et al., 2020). FCO_2 values below 0.0 for SAT are limited to central Antarctica where the overall Pliocene climate change is a cooling with respect to the PI (see Sect. 3.2), and there are no FCO_2 values below 0.0 for SST.

195 We consider uncertainty in the FCO_2 method in terms of whether there is consistent agreement between the individual models on whether CO_2 forcing or non-CO_2 forcing is the most important driver (i.e. whether $FCO_2 > 0.5$ or $FCO_2 < 0.5$). In this paper, we deem FCO_2 to be "uncertain" if four or fewer models agree on the dominant forcing (see Fig. 7, Sect. 4.1).

In checking for non-linearity, we consider an additional PlioMIP2 simulation that tests the effect of Pliocene boundary conditions with PI-level CO_2 concentration (Eoi^{280}). The sum contributions of CO_2 and non-CO_2 factors relative to the total
200 Eoi^{400}-E^{280} anomaly is close to zero (Eq. 2; Supplementary Fig. 1 (S1)), meaning that any factors not considered in these experiments – i.e. anything other than CO_2 concentration, changes to ice sheets, orography and/or vegetation – are unlikely to be a dominant cause of change. Non-linearity is tested for in the four models which had reported Eoi^{280} results by the time of

compiling this study: CCSM4-UoT, COSMOS, HadCM3 and MIROC4m. Additional checks with the other models would likely further confirm the linearity, and highlights the utility in more modelling groups completing the forcing factorisation experiments in PlioMIP2 and future phases.

$$(Eoi^{400} - E^{280}) - [(E^{400} - E^{280}) + (Eoi^{280} - E^{280})] \approx 0 \tag{2}$$

2.4. Energy balance analysis

Results from the FCO_2 method are compared to an energy balance analysis using the methodology of Hill et al. (2014). This methodology was developed from the factorisation methodology of Heinemann et al. (2009) and Lunt et al. (2012) and assumed that the change in SAT was largely driven by CO_2, orography, ice sheets and vegetation and that any other changes (such as soils or lakes) had a negligible impact:

$$\Delta T = dT_{CO_2} + dT_{orog} + dT_{ice} + dT_{veg} \tag{3}$$

In the Hill et al. (2014) methodology, the temperature at each latitude in a GCM experiment is given by:

$$T = \left(\frac{SW_{TOA}^{\downarrow}(1-\alpha) - H}{\varepsilon\sigma}\right)^{1/4} \equiv T(\varepsilon, \alpha, H) \tag{4}$$

with the temperature anomaly approximated by a linear combination of contributions from changes in emissivity (ΔT_{ε}), albedo (ΔT_{α}) and heat transport (ΔT_H). Temperature changes due to emissivity and albedo can be further separated to include changes attributed to the impact of atmospheric greenhouse gases ($\Delta T_{gg\varepsilon}$), clouds (through impacts on emissivity, $\Delta T_{c\varepsilon}$, and albedo, $\Delta T_{c\alpha}$), and clear sky albedo ($\Delta T_{cs\alpha}$). The effect of changes in temperature due to topography (ΔT_{topo}) is also important to consider when comparing the Pliocene to the PI where specific details differ (Dowsett et al., 2016).

$$\Delta T \approx \Delta T_{gg\varepsilon} + \Delta T_{c\varepsilon} + \Delta T_{c\alpha} + \Delta T_{cs\alpha} + \Delta T_H + \Delta T_{topo} \tag{5}$$

where

$$\Delta T_{gg\varepsilon} = T(\varepsilon_{cs}, \alpha, H) - T(\varepsilon'_{cs}, \alpha, H) - \Delta T_{topo} \tag{6}$$

and

$$\Delta T_{topo} = \Delta h \cdot \gamma \tag{7}$$

in which Δh is the change in topography (Pliocene-PI) and γ is a constant atmospheric lapse rate ($\approx$5.5 K km^{-1}, Yang and Smith, 1985; Hill et al., 2014).

This more approximate methodology is chosen over the further modified methodology of Feng et al. (2017) – in which an amended approximate partial radiative perturbation method was applied to calculate cloud-sky albedo more accurately in polar regions, and zonal heat transport was separated into atmosphere and ocean components – as it was used to assess the PlioMIP1 ensemble thus provides directly comparable outputs.

Six of the seven models for which FCO_2 is quantified are considered in the energy balance analysis; IPSLCM5A2 is excluded because the required fields were not available for this model. Model-specific topography files are used as they were implemented in the individual model E^{280} and Eoi^{400} experiments to minimise uncertainties that may arise due to different

implementation methods, and the energy balance components are compared to the simulated temperature change and outputs

235 of the FCO_2 method. The multi-model mean (MMM) energy balance is calculated using the MMM of each of the individual components:

$$\overline{\Delta T} \approx \overline{\Delta T_{gg\varepsilon}} + \overline{\Delta T_{c\varepsilon}} + \overline{\Delta T_{c\alpha}} + \overline{\Delta T_{cs\alpha}} + \overline{\Delta T_H} + \overline{\Delta T_{topo}} \tag{8}$$

Comparing the SAT outputs of the energy balance analysis with outputs of the FCO_2 method on SAT allow the accuracy of our novel method to be assessed, and also aids the interpretation of, and adds nuance to, the FCO_2 results. In order to assess

240 the accuracy of the simple linear estimate and to further validate the FCO_2 method, we compare $\Delta T_{gg\varepsilon}$ to the E^{400}-E^{280} SAT anomaly, and the sum of $\Delta T_{c\varepsilon}$, $\Delta T_{c\alpha}$, $\Delta T_{cs\alpha}$, ΔT_H and ΔT_{topo} to the Eoi^{400}-E^{400} SAT anomaly.

3. Results

3.1. Energy balance analysis

The Eoi^{400}-E^{280} energy balance analysis unravels the relative contributions of CO_2, topography, cloud emissivity, clear sky

245 albedo and heat transport to the Eoi^{400}-E^{280} SAT anomaly (Fig. 2). The energy balance analysis for the sub-group of PlioMIP2 models presented here supports the findings of the PlioMIP1 ensemble presented in Hill et al. (2014): clear sky albedo is the dominant driver of warming and polar amplification in the high-latitudes, and greenhouse gas emissivity is the dominant driver in the low-latitudes. The zonal influence of CO_2 on Pliocene warming also appears relatively consistent across latitudes as in Hill et al. (2014); there is some amplification at high-latitudes, particularly the Northern Hemisphere, but this amplification is

250 smaller than that seen for other energy balance components.
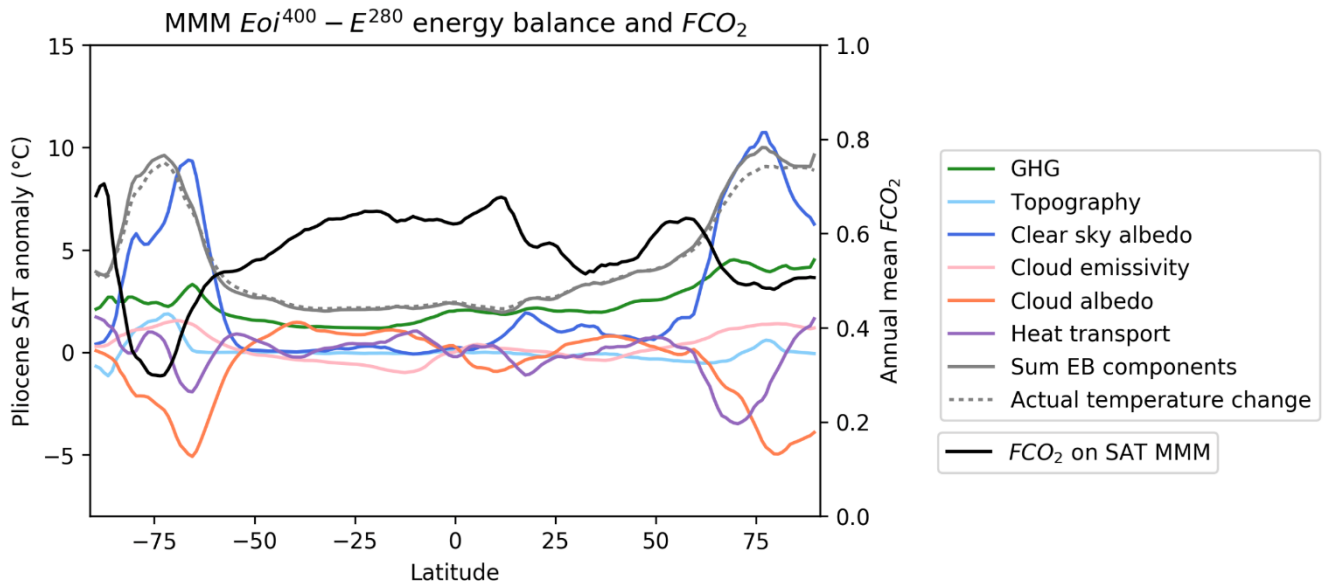
Figure 2: The MMM Eoi^{400}-E^{280} energy balance with the FCO$_2$ of the SAT MMM. The MMM includes HadCM3, COSMOS, CCSM4-UoT, CESM2, MIROC4m and NorESM1-F for both the energy balance and FCO$_2$ (IPSLCM5A2 is excluded because the required fields were not available for the energy balance analysis). The degree of Pliocene warming attributable to each energy balance component at each degree latitude is shown and the sum of the energy balance terms (solid grey line) agrees well with the simulated temperature change (dashed grey line). The FCO$_2$ of the SAT MMM is shown in the solid black line with a separate axis to compare to the energy balance.

The FCO$_2$ method provides an alternative estimate for the relative contribution of CO$_2$ to changes in SAT compared to the energy balance analysis. FCO$_2$ is lower than the greenhouse gas contribution as computed in the energy balance analysis at the high-latitudes (with the exception of the very high latitudes in the Southern Hemisphere) where there is a greater contribution from clear sky albedo and topography. Conversely, it is higher in the mid- and low-latitudes where CO$_2$ is the dominant energy balance component.

The energy balance analysis provides more nuance on the specific drivers of change than the FCO$_2$ method, which only indicates whether warming is due to CO$_2$ forcing or non-CO$_2$ forcing. Using the energy balance analysis in tandem with FCO$_2$, we are able to understand which component/s within the encompassing "non-CO$_2$" category is/are most influential. For example, the energy balance analysis highlights how clear sky albedo has the largest influence on Pliocene warming in the high-latitudes, where the FCO$_2$ method suggests that non-CO$_2$ factors are important. Furthermore, the energy balance analysis helps to explain the reasons for FCO$_2$ values above 1 for SAT; for example, although only at a zonal scale, the energy balance analysis shows that topography acts to lower SAT at the South Pole. However, the FCO$_2$ method provides spatial nuance not possible with the energy balance analysis (see Sect. 4.1).

The energy balance analysis can also be compared with the E^{400}-E^{280} and Eoi^{400}-E^{400} SAT anomalies (Fig. 3). The greenhouse gas energy balance component ($\Delta T_{gg\varepsilon}$) is seen to be in good agreement with the E^{400}-E^{280} SAT anomaly (Fig. 3a), with a global mean increase in SAT of 1.97°C and 1.85°C respectively. The energy balance component shows more variability and uncertainty between models than the E^{400}-E^{280} anomaly and also shows more zonal variation.
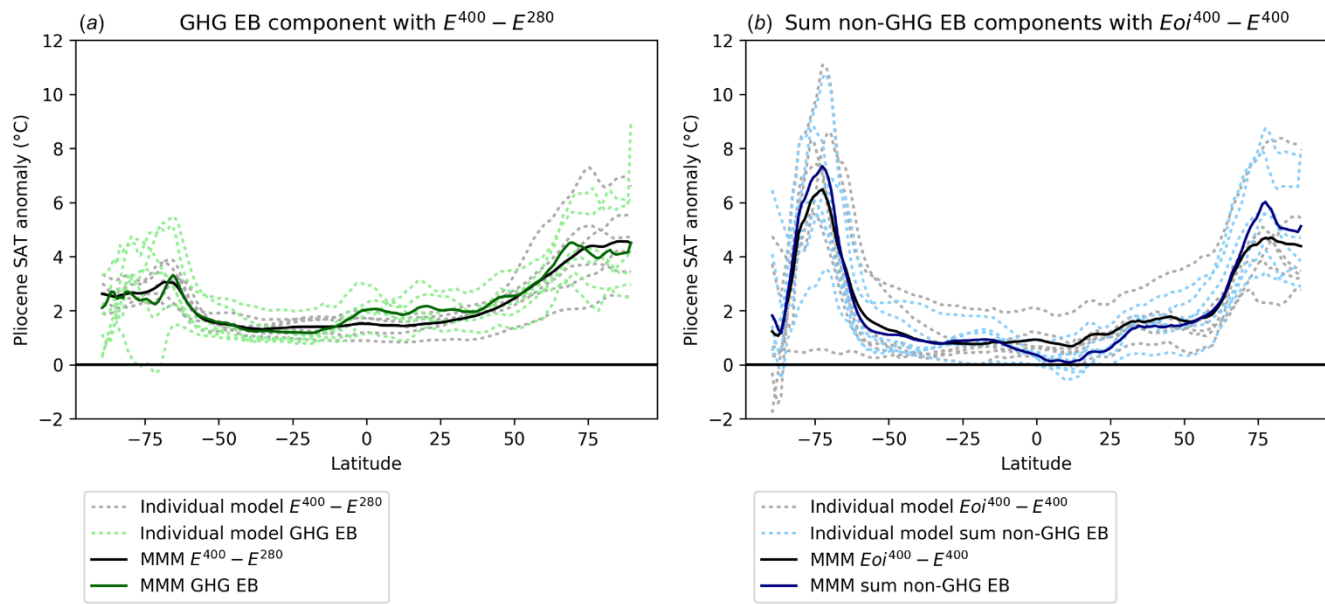
275

Figure 3: Comparison of the greenhouse gas (GHG) energy balance component ($\Delta T_{gg\epsilon}$) and the E^{400}-E^{280} SAT anomaly (a) and equivalent comparison of the sum of non-greenhouse gas energy balance components and the Eoi^{400}-E^{400} anomaly (b). The MMM is shown in a solid line and individual models by dotted lines, representing uncertainty between models.

The sum of the non-greenhouse gas energy balance components is also seen to be in good agreement with the Eoi^{400}-E^{400}

280 anomaly (Fig. 3b), with a global mean increase in SAT of 1.38°C and 1.49°C respectively. There is more uncertainty between models for the Eoi^{400}-E^{400} anomaly, highlighting the different implementations of ice sheets and land-sea masks in the Eoi^{400} experiment.

That the absolute anomalies and energy balance components agree provides an additional argument for the accuracy and usefulness of the simple linear estimations used in the FCO$_2$ method, and hence enables the first estimates of the drivers of

285 SST (Sect. 3.3) and precipitation (Sect. 3.4), as well as more spatially detailed estimates of the drivers of SAT (Sect. 3.2).

3.2. Surface air temperature

The MMM Eoi^{400}-E^{280} global mean SAT anomaly is 3.2°C, equal to the anomaly of the PlioMIP2 ensemble (Haywood et al., 2020). The range is also equal to the PlioMIP2 ensemble, with end members NorESM1-F and CESM2 simulating the smallest (1.7°C) and largest (5.2°C) Eoi^{400}-E^{280} anomalies respectively (Haywood et al., 2020). Warming occurs in all regions and is

290 amplified in the high-latitudes, except for an isolated region of cooling in central Antarctica (Fig. 4a).
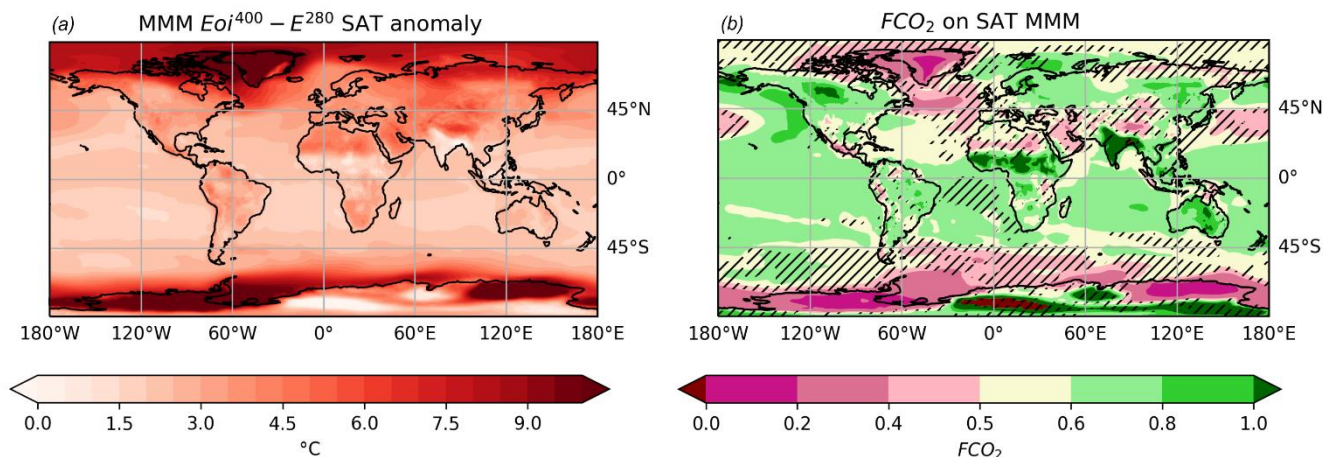
Figure 4: MMM Eoi^{400} – E^{280} SAT anomaly (a) and FCO$_2$ of the MMM for SAT (b). Hatching in (b) represents where there is no consistent agreement between models on whether CO$_2$ forcing or non-CO$_2$ forcing is the most important (i.e. whether FCO$_2$ > 0.5 or FCO$_2$ < 0.5).

295 The MMM global mean FCO$_2$ is 0.56 (individual model range 0.40-0.70; Fig. S2), meaning 56% of the SAT change is due to CO$_2$ forcing. FCO$_2$ varies around the globe (Fig. 4b): CO$_2$ is the most important forcing in large areas of the low latitudes and, predictably, becomes less important in the high latitudes due to the significant changes in ice sheets and orography in the Pliocene. FCO$_2$ is found to be similar over land and ocean, with mean values of 0.58 and 0.56 respectively.

Many areas of highly dominant CO$_2$ forcing (FCO$_2$ 0.8-1.0) are found on land: over central Africa, the Indian subcontinent,
300 and parts of Australia, Antarctica and North America. Parts of these areas have FCO$_2$ values above 1.0, indicating where non-CO$_2$ forcing acts in the opposite direction to the overall signal. However, high FCO$_2$ is also seen in the Pacific Ocean off the western coast of North America and the Barents Sea south of Svalbard.

There is a small region in the North Atlantic off the eastern coast of North America where non-CO$_2$ forcing is dominant (FCO$_2$ 0.2-0.4) but regions where non-CO$_2$ forcing is highly dominant (FCO$_2$ 0.0-0.2) are mostly limited to Antarctica and Greenland,
305 evidencing the role of changes to orography and ice sheets in polar amplification in the Pliocene. In central Antarctica there is also a region where FCO$_2$ is below 0.0, indicating where CO$_2$ forcing is acting to warm the climate against an overall signal of cooling.

The FCO$_2$ method shows CO$_2$ to be the most important forcing overall but there is also a significant contribution from non-CO$_2$ forcing which should not be overlooked, particularly if we are to learn from the Pliocene as an analogue for the future.
310 Regions of uncertainty are generally found where the dominant forcing is mixed (FCO$_2$ 0.4-0.6) but there is also uncertainty in some regions of dominant and highly dominant CO$_2$ forcing (FCO$_2$ 0.6-1.0), including central and eastern Antarctica, the Barents Sea and isolated regions of central Africa and of the Indian subcontinent (Fig. 4b). Other notable regions of uncertainty include the North Atlantic and northwest Pacific, consistent with the findings of Hill et al. (2014); however, in our analysis of PlioMIP2 simulations we find that the northern mid-latitudes appear to have more certainty than in the PlioMIP1 ensemble.

3.3. Sea surface temperature

The MMM Eoi[400]-E[280] global mean SST anomaly is 2.3°C, again equal to the global mean anomaly of the PlioMIP2 ensemble. The anomaly also sits relatively central to the PlioMIP2 ensemble range of 1.3-3.9°C (Haywood et al., 2020). Warming is seen in all ocean basins with amplification in the high-latitudes, particularly in the Labrador Sea and North Atlantic (Fig. 5a).
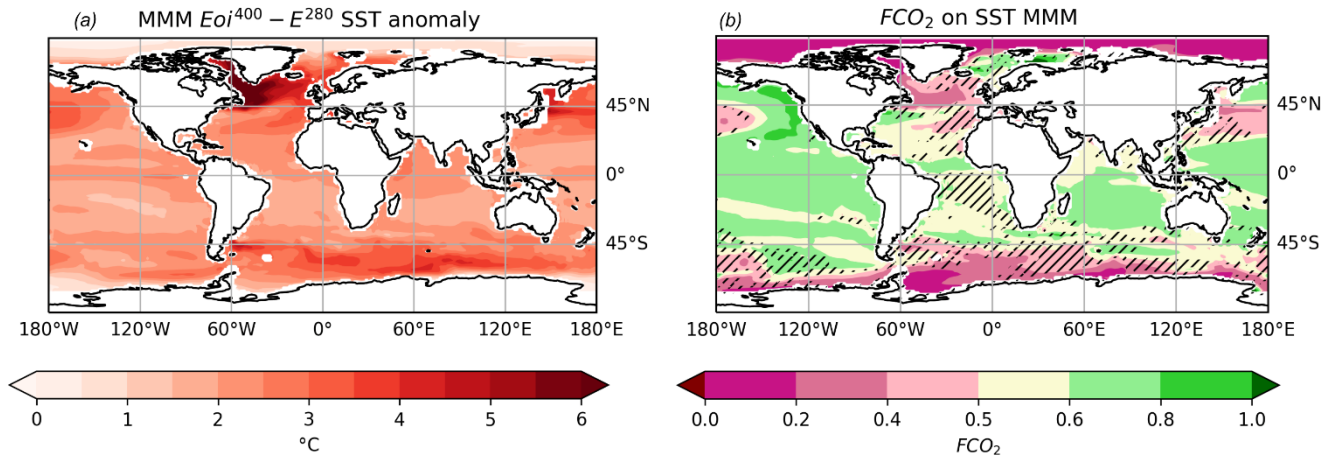
Figure 5: MMM Eoi[400] – E[280] SST anomaly (a) and FCO_2 of the MMM for SST (b). IPSLCM5A2 is excluded from SST analysis due to limited data availability. Hatching in (b) represents where there is no consistent agreement between models on whether CO_2 forcing or non-CO_2 forcing is the most important (i.e. whether $FCO_2 > 0.5$ or $FCO_2 < 0.5$).

The MMM global mean FCO_2 is 0.56 (individual model range 0.40-0.76; Fig. S3), meaning 56% of the SST change is due to CO_2 forcing. The MMM global mean FCO_2 on SST is the same as the MMM global mean FCO_2 on SAT and there are comparable spatial features at low- and mid-latitudes. On the other hand, FCO_2 on SST is significantly lower than on SAT at high-latitudes (Fig. 5b), indicating where changes in orography and ice sheets, and feedbacks including sea ice, have a much larger influence on SST than they have on SAT.

Non-CO_2 forcing is dominant or highly dominant (FCO_2 0.0-0.4) in the Arctic Sea, and dominant in much of the Southern Ocean. SST in the South Atlantic is also more strongly driven by non-CO_2 forcing than for SAT in the region, perhaps indicating a change in ocean circulation driven by these non-CO_2 forcings consistent with previous work (e.g. Hill et al., 2017). No regions of FCO_2 below 0.0 are seen.

The amplified warming seen in the Labrador Sea and North Atlantic appears to be predominantly driven by non-CO_2 forcing (FCO_2 0.2-0.4), but the warming pattern also extends to regions where forcing is mixed (FCO_2 0.4-0.6) or, south of Svalbard, where forcing is even dominated by CO_2 (FCO_2 0.6-0.8).

Regions of uncertainty in FCO_2 on SST largely mirror those for SAT over the sea surface and are predominantly found in regions of mixed forcing (FCO_2 0.4-0.6), and in the mid- and southern high-latitudes. Unlike for SAT, SSTs in the Arctic Ocean show good agreement that non-CO_2 forcing is highly dominant (FCO_2 0.0-0.2). This difference in consistency between FCO_2 on SAT and FCO_2 on SST might relate to the different distributions of sea ice between models.

3.4. Precipitation

340 The MMM Eoi^{400}-E^{280} precipitation anomaly is 0.18 mm day^{-1} or 6.4% compared to the PlioMIP2 ensemble value of 7% (range 2-13%; Haywood et al., 2020).

Particularly large increases in precipitation are seen in northern Africa and the Middle East, as well as over Greenland and parts of Antarctica (Fig. 6a). The MMM spatial pattern of precipitation change is more complex than that seen for SAT and SST but is representative of the whole PlioMIP2 ensemble (Fig. 6a; Fig. 1d).
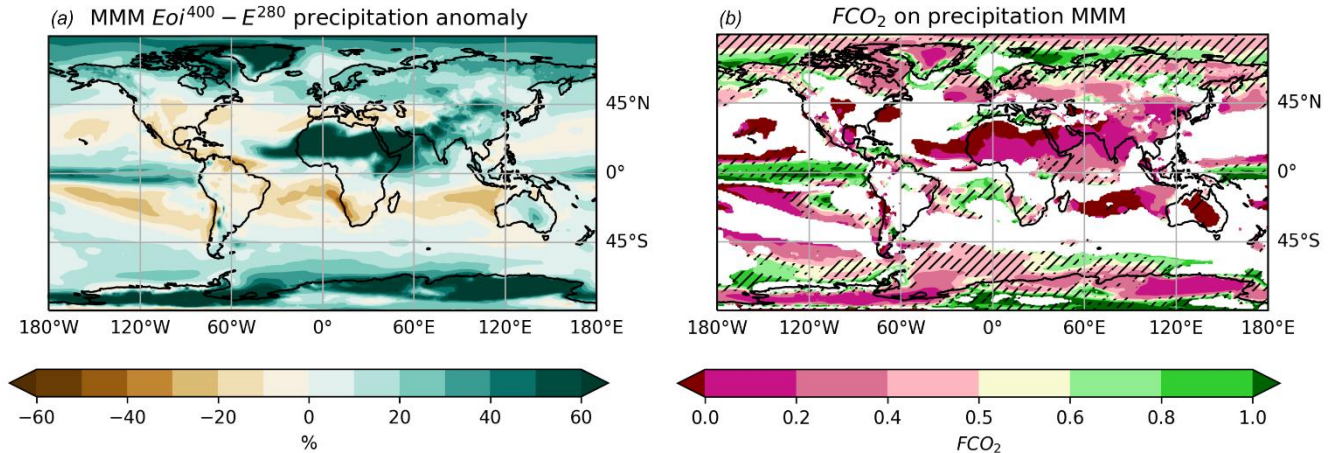
345

Figure 6: MMM Eoi^{400} – E^{280} precipitation anomaly (a) and FCO$_2$ of MMM for precipitation (b). In (b), regions of Eoi^{400}-E^{280} precipitation change less than 10% are masked (white) and hatching represents where there is no consistent agreement between models on whether CO$_2$ forcing or non-CO$_2$ forcing is the most important (i.e. whether FCO$_2$ > 0.5 or FCO$_2$ < 0.5).

The spatial pattern of FCO$_2$ on precipitation is also more complex than that seen for SAT and SST; areas of percentage change
350 less than 10% are masked in white to increase clarity and reduce noise (Fig. 6b). The MMM global mean FCO$_2$ is 0.51 (individual model range 0.39-0.69; Fig. S4), meaning CO$_2$ forcing causes 51% of the change in global mean precipitation and so non-CO$_2$ forcing plays a slightly more important role in changes in precipitation than is the case for SAT and SST. For precipitation, there is a large difference in FCO$_2$ over land compared to oceans, with mean values of 0.23 and 0.58 respectively; non-CO$_2$ forcing is much more important over land.

355 The largest increases in precipitation are generally driven by non-CO$_2$ forcing, seen over northern Africa and the Indian subcontinent (see Feng et al., 2022), Greenland, and parts of eastern and western Antarctica. Parts of northern Africa have FCO$_2$ values below 0.0, indicating that CO$_2$ is acting to limit this increase in precipitation. FCO$_2$ values below 0.0 are also seen in central Australia, central North America and parts of the tropical Indian, Atlantic and Pacific Oceans, where the signals in precipitation anomaly are both positive and negative.

360 Non-CO$_2$ forcing is also dominant (FCO$_2$ 0.2-0.4) or highly dominant (FCO$_2$ 0.0-0.2) in some regions of precipitation decrease, including the tropical south Pacific, and the regions west of the maritime continent and off the eastern coast of North America.

There are also regions where FCO_2 is above 1.0 in parts of central and eastern Antarctica, the tropical Pacific, the Barents Sea, and a small area in both the Bering Sea and the Arctic Ocean north of Alaska. These are mostly regions of small precipitation increase, indicating that non-CO_2 forcing acts to decrease precipitation despite the overall increase.

365 Spatial changes appear predominantly driven by non-CO_2 forcing, whereas CO_2 forcing has a more muted and widespread effect. The overall effect of CO_2 is an increase in global mean precipitation, although we see both increases and decreases in precipitation regionally which appear attributable to non-CO_2 forcing such as changes in orography, ice sheets and/or vegetation. That such local changes have a notable effect on the Pliocene precipitation anomaly may limit the degree to which we can use the Pliocene as a precipitation analogue for our warmer future.

370 There is more uncertainty between models for FCO_2 on precipitation than for SAT and SST. Uncertainty is seen in regions of both mixed forcing (FCO_2 0.4-0.6) and dominant or highly dominant CO_2 forcing (FCO_2 0.6-1.0). Regions predominantly driven by non-CO_2 forcing (FCO_2 0.0-0.4) show better agreement between models, suggesting that the impact of non-CO_2 forcing is more robustly represented in the PlioMIP2 ensemble than the impact of CO_2 on precipitation.

4. Discussion

375 **4.1. FCO_2 method**

The FCO_2 method has been validated by comparing outputs to the energy balance analysis and presents a great opportunity to expand our understanding of climate drivers in the Pliocene and beyond.

We devised a novel method to quantitatively estimate the drivers of Pliocene SST and precipitation. This method can be applied to other climate variables, with relative ease and little computational cost, and to other ensembles of models beyond PlioMIP2.

380 Aided by comparison to the energy balance analysis, the FCO_2 method provides a complete view of drivers of Pliocene climate at both global and regional scales; in particular, contributions of CO_2 vs. non-CO_2 forcing for SAT, SST and precipitation on local and regional scales are revealed. We also show how comparison to the energy balance analysis adds insight into feedbacks and other such indirect effects of CO_2 forcing which the FCO_2 method does not capture.

This work has also highlighted the value and accuracy of using the E^{400}-E^{280} and Eoi^{400}-E^{400} SAT anomalies as an estimate for

385 $\Delta T_{gg\varepsilon}$ and the sum of the non-greenhouse gas components in energy balance analyses respectively. This shows that, while exact information on the drivers of temperature still depend on the application of a more elaborated and computationally expensive set of sensitivity simulations, a good degree of knowledge may be derived by applying a much smaller number of simulations. This is not only more economic, but it may also increase the number of modelling groups that take part in future model intercomparison studies of the kind that we have presented here. The FCO_2 method requiring a smaller number of

390 simulations compared to the energy balance analyses has allowed for a larger ensemble of models to be assessed than previously in PlioMIP2.

The FCO$_2$ method also allows for an assessment of the uncertainty between models for the drivers of the different climate parameters by comparing where there is/not consistent agreement on the forcing, i.e. whether FCO$_2 > 0.5$ or FCO$_2 < 0.5$ (Fig. 7).
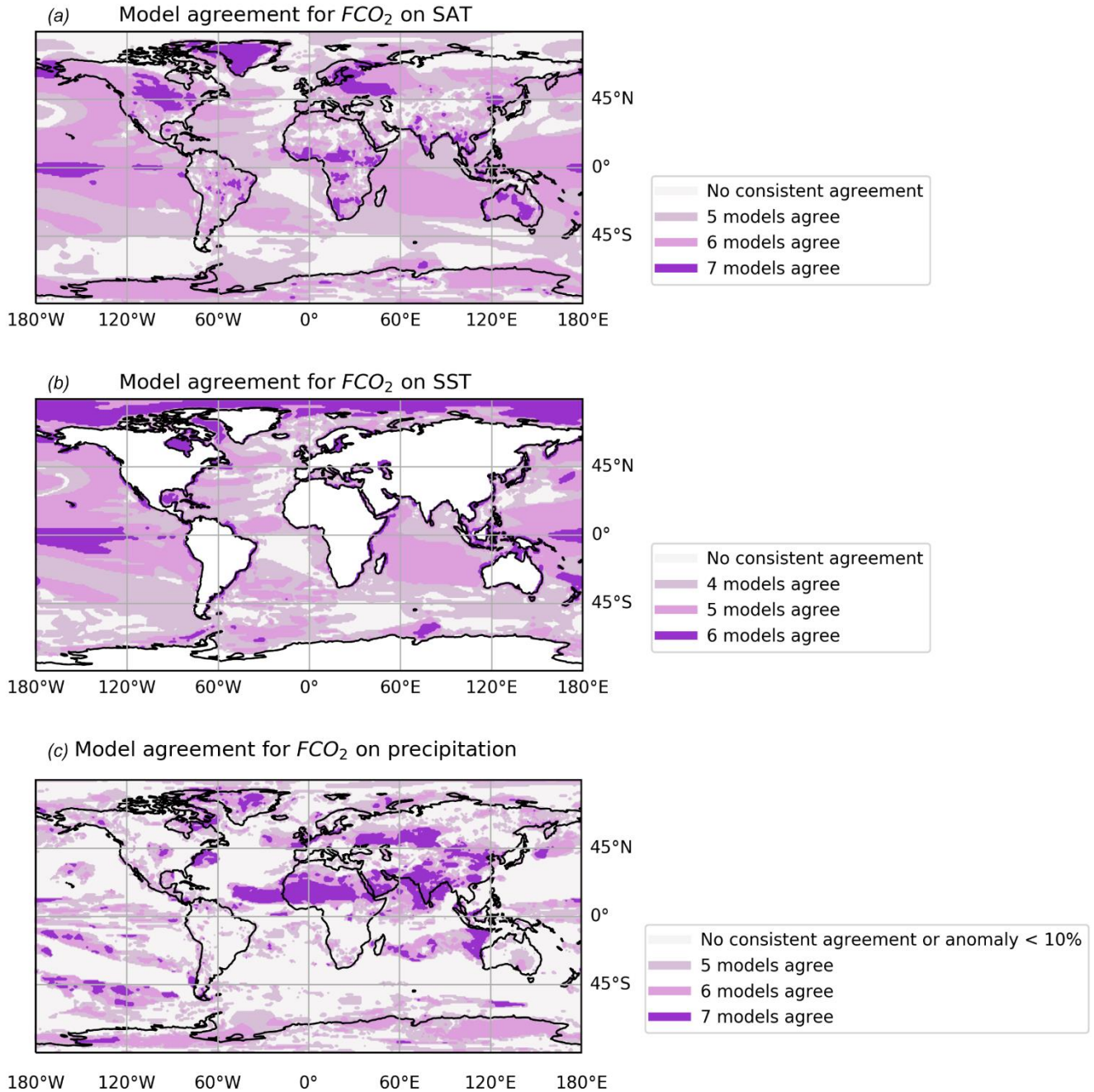
395

Figure 7: The level of agreement between models included in the FCO$_2$ analysis, showing where models agree on the dominant forcing shown by the FCO$_2$ method (i.e. whether FCO$_2 > 0.5$ or FCO$_2 < 0.5$). All seven models (CCSM4-UoT, CESM2, COSMOS,

400

There is consistent agreement between five or more models on the dominant forcing of SAT over 74.8% of the Earth's surface (Fig. 7a), of SST over 46.5% of the ocean surface (Fig. 7b), and of precipitation over 66.8% of regions with an Eoi^{400}-E^{280} anomaly greater than 10% (Fig. 7c). If the criteria for 'consistency' is extended to four or more models for SST – for which only six models are assessed – the area in agreement increases to 83.1%.

405   Though FCO_2 on precipitation is not the most consistent, in regions of agreement it is more common for all seven models to agree: all seven models agree on the dominant forcing in 13.8% of the area assessed for precipitation, compared to 4.6% for SAT. All six models agree on the dominant forcing for SST over 11.4% of the ocean surface.

4.2. Drivers of Pliocene climate

Using the FCO_2 method, CO_2 forcing was found to be the largest cause of SAT, SST and precipitation change in the Pliocene 410   with global mean MMM FCO_2 values of 0.56, 0.56 and 0.51 respectively.

The percentage of SAT change predominantly driven by CO_2 using the FCO_2 method, 56%, is comparable to estimates from previous studies, including specific comparisons for HadCM3 (Lunt et al., 2012), CCSM4-UoT (Chandan and Peltier, 2018) and COSMOS (Stepanek et al., 2020), as well as the PlioMIP1 ensemble (Hill et al., 2014).

Lunt et al. (2012) concluded that 48% of warmth simulated in HadCM3 was caused by CO_2 when the atmospheric concentration 415   was set to 400 ppm, decreasing to 36% at 350 ppm and increasing to 61% at 450 ppm. Exploring the effect of different atmospheric CO_2 concentrations in this way would be possible using the FCO_2 method but is constrained by the experiments set out in the PlioMIP2 experimental design; further division of forcing factorisation experiments and/or more models conducting these experiments (particularly the separated Eo^{400} and Ei^{400} experiments) may be a fruitful addition looking to PlioMIP3.

420   Using the FCO_2 method, 59% of the Pliocene SAT anomaly is caused by CO_2 in HadCM3 (global mean FCO_2 = 0.59; Fig. S2d). This is higher than the estimate of 48% in Lunt et al. (2012) but it is important to note the development in boundary conditions from PRISM2 (used in Lunt et al., 2012) and PRISM4 (used in PlioMIP2) which will account for some of the difference, as well as the difference in methodology.

The percentage of warming predominantly caused by CO_2 using the FCO_2 method in CCSM4-UoT, 52% (global mean FCO_2 425   = 0.52; Fig. S2a), is also higher than the ~45% estimated in Chandan and Peltier (2018) using the nonlinear factorisation methodology of Lunt et al. (2012).

On the other hand, the FCO_2 method slightly underestimates the contribution of CO_2 in COSMOS compared to the full factorisation in Stepanek et al. (2020). The global mean FCO_2 for COSMOS is found to be 0.64 (64% CO_2 contribution equivalent), compared to 66% in Stepanek et al. (2020). This may reflect the incorporation of some vegetation feedback in the

430 E^{400}-E^{280} anomaly used to calculate FCO_2 given that COSMOS ran with dynamic vegetation, but additional simulations of COSMOS using prescribed vegetation would be needed to explore this further.

In validating the FCO_2 method, this paper has also presented the first energy balance results for a subgroup of models in the PlioMIP2 ensemble. By using the same methodology as Hill et al. (2014) in the framework of PlioMIP1, our results based on PlioMIP2 experiments become directly comparable and similar trends are seen: greenhouse gas emissivity is dominant in

435 driving warming in the tropics while all forcing components become important in the high-latitudes, with polar amplification particularly driven by clear-sky albedo. The relative dominance of CO_2 forcing in the low- and mid-latitudes compared to the high-latitudes is also seen in the FCO_2 results.

We find notable variation of results based on the FCO_2 method between individual climate models, though the level of variation is consistent between the three climate variables assessed. Despite having the highest ECS value in the PlioMIP2 ensemble

440 (5.3°C; Gettelman et al., 2019; Haywood et al., 2020), CESM2 has the lowest FCO_2 for all three variables at 0.40 for SAT and SST, and 0.39 for precipitation. This further highlights the sensitivity of CESM2 to all changes in boundary conditions, not just CO_2 (Feng et al., 2020).

The model with the highest global mean FCO_2 differs between variables. NorESM1-F has the highest FCO_2 on SAT at 0.70, while COSMOS has the highest FCO_2 on SST and precipitation at 0.76 and 0.69, respectively. NorESM1-F has the lowest

445 ECS value in the PlioMIP2 ensemble (2.3°C), but COSMOS has the third highest (4.7°C; Haywood et al., 2020). Though it might seem intuitive that models with a higher ECS would also have a higher FCO_2, the relationship between FCO_2 and climate sensitivity can be better described by the ESS to ECS ratio which captures the relatively short-term influence of CO_2 compared to longer-term responses of the Earth System (Fig. 8). Perhaps an artefact of the reduced sample size (six models compared to seven), the ESS to ECS ratio correlates best with the global mean FCO_2 on SST ($R^2 = 0.71$), followed by SAT ($R^2 = 0.50$) and

450 precipitation ($R^2 = 0.41$). This relationship would be better explored with a greater sample size, again reinforcing the usefulness of model groups completing the forcing factorisation experiments ahead of PlioMIP3.
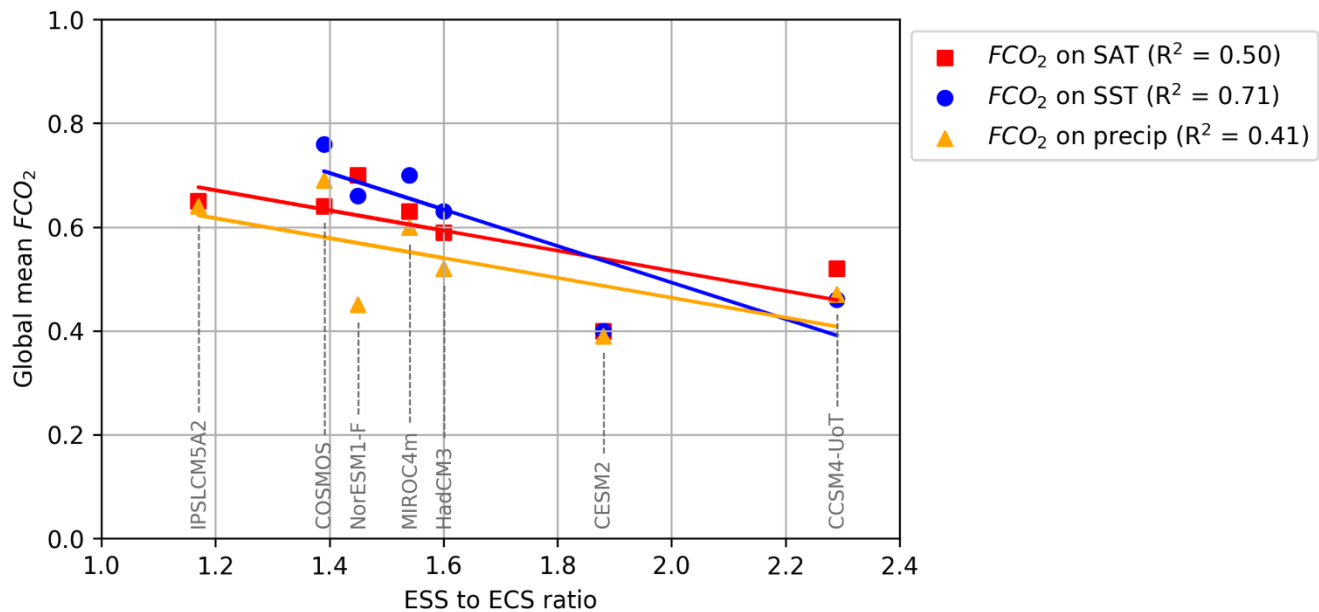
Figure 8: The relationship between the ESS to ECS ratio and global mean FCO_2. IPSLCM5A2 is excluded from the SST analysis due to limited data availability.

4.3. The Pliocene as an analogue for the future?

A significant motivation behind studying the Pliocene is its use as a potential palaeoclimate analogue for the near-term future. If the Pliocene is to be an accurate and useful analogue for the future, it stands that the drivers of its climate should also be analogous to those driving current anthropogenic climate change alongside its large-scale climate features.

The FCO_2 method allows us to answer the question of how analogous the drivers of Pliocene climate are to those of the near-term future in more detail than has been possible previously. It also allows us to consider this question in terms of SST and precipitation change for the first time.

Current warming is predominantly driven by anthropogenic greenhouse gas emissions (Eyring et al., 2021). The FCO_2 results presented here show that, although CO_2 was the most important forcing in the Pliocene, it drove only 56% of SAT and SST change and 51% of precipitation change in the ensemble of PlioMIP2 models considered in this study. Therefore, 44% of SAT and SST change and 49% of precipitation change was driven by non-CO_2 forcing.

While we are already experiencing some shifts towards a Pliocene-like state for some of these non-CO_2 components – such as the greening of the Arctic (e.g. Myers-Smith et al., 2020) – other changes will take longer to fully materialise as the system equilibrates to higher levels of anthropogenic CO_2 forcing, with implications on the accuracy and utility of the Pliocene as a palaeoclimate analogue for near-term future climate. Regions of high FCO_2 in the Pliocene are likely to be more analogous for the immediate and near-term future for as long as atmospheric CO_2 concentration remains similar to Pliocene levels (~400

ppm), whereas regions of lower FCO_2 may become more analogous in the longer-term future as the full, equilibrated effects of changes to ice sheets and vegetation are experienced.

This raises two important points. The first highlights the importance of understanding the broader Earth System feedbacks of an atmospheric CO_2 concentration similar-to-modern, particularly as anthropogenic greenhouse gas emissions continue to increase (Dhakal et al., 2022) with the likelihood of soon moving beyond Pliocene levels (~400 ppm; Meinshausen et al., 2020). The E^{400}-E^{280} SAT anomaly shows that, for the subgroup of seven PlioMIP2 models assessed here, CO_2 forcing alone was responsible for 1.8°C of the total 3.2°C increase seen in the Eoi^{400}-E^{280} global mean SAT anomaly. We have experienced around 1.1°C of warming relative to the PI with an atmospheric CO_2 concentration of around 410 ppm (Gulev et al., 2021). The Pliocene – being around 3°C warmer than the PI in quasi-equilibrium with a CO_2 concentration ~400 ppm (e.g. Haywood et al., 2020) – shows that more warming is to come as the system equilibrates with the anthropogenic greenhouse gas forcing that has already been emitted, even if greenhouse gas emissions were to stop immediately.

The second point highlights the need to define what we mean by palaeoclimate analogue in the situation of our research. This should include consideration of the climate variable/s, region/s and time frame/s of interest (including whether the system is in a transient or equilibrium state, with implications for modes of variability (e.g. Bonan et al., 2022)), as well as the level of accuracy deemed to be 'analogous'. Our results also highlight the need to consider the nature of the climate forcing.

Burke et al. (2018) explore the spatial and temporal variations of past warm periods as analogues for different potential climate futures by comparing six geohistorical periods (PI, Historical, Holocene, Last Interglacial, Pliocene and Eocene) to Representative Concentration Pathway (RCP) 4.5 and RCP8.5. They find the Pliocene to be the best analogue for our near-term future under RCP4.5, though just because the Pliocene is one of the best palaeoclimate analogues does not necessarily mean that it is a perfect analogue without constraints or limitations.

Future work could expand the work of Burke et al. (2018) using the FCO_2 method to incorporate additional climate variables, which would also allow for discussion on the analogous nature of the drivers of these variables.

The results presented here highlight that, though there may be similarities in large-scale features of Pliocene and near-term future climate, the drivers of these features may be less similar or analogous and drawing any such conclusions must be done so with caution and account for the significant contributions of non-analogous forcings.

5. Summary and future work

We have introduced a novel method for assessing the influence of different forcing factors in the Pliocene. The FCO_2 method only requires a small subset of forcing factorisation experiments of PlioMIP2 and can be applied to multiple climate variables, and to a large ensemble of models with little computational complexity and cost. We have validated the FCO_2 method by comparing the results for SAT to an energy balance analysis using the methodology of Hill et al. (2014), which was originally used to assess the drivers of warming in the PlioMIP1 ensemble.

For the first time, we have quantitatively estimated the effect of CO_2 forcing on Pliocene SST and precipitation. CO_2 is found to be the most important forcing of global mean SAT, SST and precipitation with global mean FCO_2 values of 0.56 (individual model range 0.40-0.70), 0.56 (individual model range 0.40-0.76) and 0.51 (individual model range 0.39-0.69) respectively.

505 Though CO_2 is the most important forcing, there remains significant contributions from non-CO_2 forcing and such changes in orography, ice sheets and/or vegetation are found to have a greater impact in driving regional spatial changes. The influence of these non-CO_2 forcings must not be overlooked, particularly in the context of using the Pliocene as an analogue for the near-term future.

Outputs from the FCO_2 method also provide new insights relevant to the palaeo-data community which could aid the

510 interpretation of proxy data and data-model comparison efforts, as well as inform estimates of climate sensitivity. These insights will be explored in a future paper. The FCO_2 method shows us which regions of the world are most (and least) influenced by CO_2 forcing, with direct implications on the interpretation of proxy data at these sites and any biases they may present. Additionally, we can also use the outputs from the FCO_2 method to suggest regions from which additional proxy data would be useful to further refine our interpretation of Pliocene climate, such as where there is uncertainty between models.

515 As we look towards the planning of PlioMIP3, our work clearly highlights the usefulness and importance of including forcing factorisation experiments that can provide us with a more detailed view of the drivers of Pliocene climate, with direct relevance to the discussion on using the Pliocene as an analogue for our warmer future.

Data availability

The data required to produce the results in this paper is available in the Supplement.

520 **Author contribution**

LEB, AMH, JCT, AMD and DJH prepared the paper with contributions from all co-authors. AAO, WLC, DC, RF, SJH, XL, WRP, NT, CS and ZZ provided PlioMIP2 experiments run with the individual models.

Competing interests

Some authors are members of the editorial board of Climate of the Past. The peer-review process was guided by an independent

525 editor, and the authors have also no other competing interests to declare.

Acknowledgements

For the purpose of open access, the author has applied a Creative Commons Attribution (CC BY) licence to any Author Accepted Manuscript version arising. Lauren E. Burton acknowledges that this work was supported by the Leeds-York-Hull

Natural Environment Research Council (NERC) Doctoral Training Partnership (DTP) Panorama under grant NE/S007458/1.

530 Julia C Tindall was supported through the Centre for Environmental Modelling and Computation (CEMAC), University of Leeds. Research by Wing-Le Chan and Ayako Abe-Ouchi was supported by JSPS Kakenhi grant no. 17H06104 (Japan) and MEXT Kakenhi grant no. 17H06323 (Japan). Christian Stepanek acknowledges support at AWI by the Helmholtz Climate Initiative REKLIM and the research program PACES-II of the Helmholtz Association. W. Richard Peltier and Deepak Chandan were supported by Canadian NSERC Discovery Grant A9627, and they wish to acknowledge the support of SciNet

535 HPC Consortium for providing computing facilities. SciNet is funded by the Canada Foundation for Innovation under the auspices of Compute Canada, the Government of Ontario, the Ontario Research Fund – Research Excellence, and the University of Toronto. Ning Tan acknowledges support from National Natural Science Foundation of China program 41907371. Aisling M. Dolan and Stephen J. Hunter were supported by the FP7 Ideas: European Research Council (grant no. PLIO-ESS, 278636). The CESM2 simulations are performed with high-performance computing support from Cheyenne

540 (doi:10.5065/D6RX99HX) provided by NCAR's Computational and Information Systems Laboratory, sponsored by the National Science Foundation. Ran Feng acknowledges support from National Science Foundation (No. 2103055). The NorESM simulations benefitted from resources provided by UNINETT Sigma2 – the National Infrastructure for High Performance Computing and Data Storage in Norway.

References

545 Bartoli, G., Hönisch, B. and Zeebe, R.E.: Atmospheric CO_2 decline during the Pliocene intensification of Northern Hemisphere glaciations, Paleoceanography, 26, PA4213, https://doi.org/10.1029/2010PA002055, 2011.

Bonan, D.B., Thompson, A.F., Newsom, E.R., Sun, S. and Rugenstein, M.: Transient and equilibrium responses to the Atlantic Overturning Circulation to warming in coupled climate models: The role of temperature and salinity, J. Climate, 35, 5173-5193, https://doi.org/10.1175/JCLI-D-21-0912.1, 2022.

550 Burke, K.D., Williams, J.W., Chandler, M.A., Haywood, A.M., Lunt, D.J. and Otto-Bliesner, B.L.: Pliocene and Eocene provide best analogs for near-future climates, P. Natl. Acad. Sci. USA, 115, 13288-13293, https://doi.org/10.1073/pnas.1809600115, 2018.

Chan, W.-L. and Abe-Ouchi, A.: Pliocene Model Intercomparison Project (PlioMIP2) simulations using the Model for Interdisciplinary Research on Climate (MIROC4m), Clim. Past, 16, 1523-1545, https://doi.org/10.5194/cp-16-1523-2020,

555 2020.

Chandan, D. and Peltier, W.R.: Regional and global climate for the mid-Pliocene using the University of Toronto version of CCSM4 and PlioMIP2 boundary conditions, Clim. Past, 13, 919-942, https://doi.org/10.5194/cp-13-919-2017, 2017.

Chandan, D. and Peltier, W.R.: On the mechanisms of warming the mid-Pliocene and the inference of a hierarchy of climate sensitivities with relevance to the understanding of climate futures, Clim. Past, 14, 825-856, https://doi.org/10.5194/cp-14-

560 825-2018, 2018.

Corvec, S. and Fletcher, C.G.: Changes to the tropical circulation in the mid-Pliocene and their implications for future climate, Clim. Past, 13, 135-147, https://doi.org/10.5194/cp-13-135-2017, 2017.

de la Vega, E., Chalk, T.B., Wilson, P.A., Bysani, R.P. and Foster, G.L.: Atmospheric CO_2 during the Mid-Piacenzian Warm Period and the M2 glaciation, Sci. Rep.-UK, 10, 11002, https://doi.org/10.1038/s41598-020-67154-8, 2020.

565   DeConto, R.M. and Pollard, D.: Contribution of Antarctica to past and future sea-level rise, Nature, 531, 591-597, https://doi.org/10.1038/nature17145, 2016.

Dhakal, S., Minx, J.C., Toth, F.L., Abdel-Aziz, A., Figueroa Meza, M.J., Hubacek, K., Jonckheere, I. G.C., Kim, Y.-G., Nemet, G.F., Pachauri, S., Tan, X.C. and Wiedmann, T.: Emissions Trends and Drivers. In IPCC, 2022: Mitigation of Climate Change. Contribution of Working Group III to the Sixth Assessment Report of the Intergovernmental Panel on

570   Climate Change [Shukla, P.R., Skea, J., Slade, R., Al Khourdajie, A., van Diemen, R., McCollum, D., Pathak, M., Some, S., Vyas, P., Fradera, R., Belkacemi, M., Hasija, A., Lisboa, G., Luz, S. and Malley, J. (eds.)]. Cambridge University Press, Cambridge, UK and New York, NY, USA., doi: 10.1017/9781009157926.004, 2022.

Dolan, A.M., Hunter, S.J., Hill, D.J., Haywood, A.M., Koenig, S.J., Otto-Bliesner, B.L., Abe-Ouchi, A., Bragg, F., Chan, W.L., Chandler, M.A., Contoux, C., Jost, A., Kamae, Y., Lohmann, G., Lunt, D.J., Ramstein, G., Rosenbloom, N.A., Sohl,

575   L., Stepanek, C., Ueda, H., Yan, Q. and Zhang, Z.: Using results from the PlioMIP ensemble to investigate the Greenland Ice Sheet during the mid-Pliocene Warm Period, Clim Past, 11, 403-424, https://doi.org/10.5194/cp-11-403-2015, 2015.

Douville, H., Raghavan, K., Renwick, J., Allan, R.P., Arias, P.A., Barlow, M., Cerezo-Mota, R., Cherchi, A., Gan, T.Y., Gergis, J., Jiang, D., Khan, A., Pokam Mba, W., Rosenfeld, D, Tierney, J. and Zolina, O.: Water Cycle Changes. In Climate Change 2021: The Physical Science Basis. Contribution of Working Group I to the Sixth Assessment Report of the

580   Intergovernmental Panel on Climate Change [Masson-Delmotte, V., Zhai, P., Pirani, A., Connors, S.L., Péan, C., Berger, S., Caud, N., Chen, Y. Goldfarb, L., Gomis, M.I., Huang, M., Leitzell, K., Lonnoy, E., Matthews, J.B.R., Maycock, T.K., Waterfield, T., Yelekçi, O., Yu, R. and Zhou, B. (eds.)]. Cambridge University Press, Cambridge, United Kingdom and New York, NY, USA., 1055-1210, doi:10.1017/9781009157896.010, 2021.

Dowsett, H.J., Barron, J.A., Poore, R.Z., Thompson, R.S., Cronin, T.M., Ishman, S.E. and Willard, D.A.: Middle Pliocene

585   paleoenvironmental reconstruction: PRISM 2. U.S. Geological Survey Open File Report 99-535, 1999.

Dowsett, H.J.: The PRISM palaeoclimate reconstructions and Pliocene sea-surface temperature, in: Perspectives on Climate Change: Marrying the Signal from Computer Models and Biological Proxies, edited by: Williams, M., Haywood, A.M., Gregory, F.J. and Schmidt, D.N., Micropalaeontological Society, Special Publications, The Geological Society, London, 459–480, 2007.

590   Dowsett, H., Robinson, M., Haywood, A., Salzmann, U., Hill, D., Sohl, L., Chandler, M., Williams, M., Foley, K. and Stoll, D.: The PRISM3D paleoenvironmental reconstruction, Stratigraphy, 7, 123-139, 2010.

Dowsett, H., Dolan, A., Rowley, D., Moucha, R., Forte, A.M., Mitrovica, J.X., Pound, M., Salzmann, U., Robinson, M., Chandler, M., Foley, K. and Haywood, A.: The PRISM4 (mid-Piacenzian) paleoenvironmental reconstruction, Clim. Past, 12, 1519-1538, https://doi.org/10.5194/cp-12-1519-2016, 2016.

595   Eyring, V., Gillett, N.P., Achuta Rao, K.M., Barimalala, R., Barreiro Parrillo, M., Bellouin, N., Cassou, C., Durack, P.J., Kosaka, Y., McGregor, S., Min, S., Morgenstern, O. and Sun, Y.: Human Influence on the Climate System. In Climate Change 2021: The Physical Science Basis. Contribution of Working Group I to the Sixth Assessment Report of the Intergovernmental Panel on Climate Change [Masson-Delmotte, V., Zhai, P., Pirani, A., Connors, S.L., Péan, C., Berger, S., Caud, N., Chen, Y. Goldfarb, L., Gomis, M.I., Huang, M., Leitzell, K., Lonnoy, E., Matthews, J.B.R., Maycock, T.K.,

600   Waterfield, T., Yelekçi, O., Yu, R. and Zhou, B. (eds.)]. Cambridge University Press, Cambridge, United Kingdom and New York, NY, USA., 423–552, doi:10.1017/9781009157896.005, 2021.

Feng, R., Otto-Bliesner, B.L., Fletcher, T.L., Tabor, C.R., Ballantyne, A.P. and Brady, E.C.: Amplified Late Pliocene terrestrial warmth in northern high latitudes from greater radiative forcing and closed Arctic Ocean gateways, Earth Planet. Sc. Lett., 466, 129-138, https://doi.org/10.1016/j.epsl.2017.03.006, 2017.

605   Feng, R., Otto-Bliesner, B.L., Xu, Y., Brady, E., Fletcher, T., Ballantyne, A.: Contributions of aerosol-cloud interactions to mid-Piacenzian seasonally sea ice-free Arctic Ocean, Geophys. Res. Lett., 46, 9920-9929, https://doi.org/10.1029/2019GL083960, 2019.

Feng, R., Otto-Bliesner, B.L., Brady, E.C. and Rosenbloom, N.: Increased Climate Response and Earth System Sensitivity From CCSM4 to CESM2 in Mid-Pliocene Simulations, J. Adv. Model. Earth. Sy., 12, e2019MS002033,

610   https://doi.org/10.1029/2019MS002033, 2020.

Feng, R., Bhattacharya, T., Otto-Bliesner, B.L., Brady, E.C., Haywood, A.M., Tindall, J.C., Hunter, S.J., Abe-Ouchi, A., Chan, W.L., Kageyama, M., Contoux, C., Guo, C., Li, X., Lohmann, G., Stepanek, C., Tan, N., Zhang, Q., Zhang, Z., Han, X., Williams, C J.R., Lunt, D.J., Dowsett, H. J., Chandan, D. and Peltier, W.R.: Past terrestrial hydroclimate sensitivity controlled by Earth system feedbacks, Nat Commun, 13, 1-11, https://doi.org/10.1038/s41467-022-28814-7, 2022.

615   Gettelman, A., Hannay, C., Bacmeister, J.T., Neale, R.B., Pendergrass, A.G., Danabasoglu, G., Lamarque, J.F., Fasullo, J.T., Bailey, D.A., Lawrence, D.M. and Mills, M.J.: High Climate Sensitivity in the Community Earth System Model Version 2 (CESM2), Geophys. Res. Lett., 46, 8329-8337, https://doi.org/10.1029/2019GL083978, 2019.

Gulev, S.K., Thorne, P.W., Ahn, J., Dentener, F.J., Domingues, C.M., Gerland, S., Gong, D., Kaufman, D.S., Nnamchi, H.C., Quaas, J., Rivera, J.A., Sathyendranath, S., Smith, S.L., Trewin, B., von Schuckmann, K. and Vose, R.S.: Changing

620   State of the Climate System. In Climate Change 2021: The Physical Science Basis. Contribution of Working Group I to the Sixth Assessment Report of the Intergovernmental Panel on Climate Change [Masson-Delmotte, V., Zhai, P., Pirani, A., Connors, S.L., Péan, C., Berger, S., Caud, N., Chen, Y. Goldfarb, L., Gomis, M.I., Huang, M., Leitzell, K., Lonnoy, E., Matthews, J.B.R., Maycock, T.K., Waterfield, T., Yelekçi, O., Yu, R. and Zhou, B. (eds.)]. Cambridge University Press, Cambridge, United Kingdom and New York, NY, USA., 287–422, doi:10.1017/9781009157896.004, 2021.

625   Guo, C., Bentsen, M., Bethke, I., Ilicak, M., Tjiputra, J., Toniazzo, T., Schwinger, J. and Otterå, O.H.: Description and evaluation of NorESM1-F: a fast version of the Norwegian Earth System Model (NorESM), Geosci. Model Dev., 12, 343-362, https://doi.org/10.5194/gmd-12-343-2019, 2019.

Gutiérrez, J.M., Jones, R.G., Narisma, G.T., Alves, L.M., Amjad, M., Gorodetskaya, I.V., Grose, M., Klutse, N.A.B., Krakovska, S., Li, J., Martínez-Castro, D., Mearns, L.O., Mernild, S.H., Ngo-Duc, T., van den Hurk, B., and J.-H. Yoon, J.-

630   H.: Atlas. In Climate Change 2021: The Physical Science Basis. Contribution of Working Group I to the Sixth Assessment Report of the Intergovernmental Panel on Climate Change [Masson-Delmotte, V., Zhai, P., Pirani, A., Connors, S.L., Péan, C., Berger, S., Caud, N., Chen, Y. Goldfarb, L., Gomis, M.I., Huang, M., Leitzell, K., Lonnoy, E., Matthews, J.B.R., Maycock, T.K., Waterfield, T., Yelekçi, O., Yu, R. and Zhou, B. (eds.)]. Cambridge University Press. In Press. Interactive Atlas available from http://interactive-atlas.ipcc.ch/, 2021.

635   Haywood, A.M., Dowsett, H.J., Otto-Bliesner, B., Chandler, M.A., Dolan, A.M., Hill, D.J., Lunt, D.J., Robinson, M.M., Rosenbloom, N., Salzmann, U. and Sohl, L.E.: Pliocene Model Intercomparison Project (PlioMIP): experimental design and boundary conditions (Experiment 1), Geosci. Model Dev., 3, 227-242, https://doi.org/10.5194/gmd-3-227-2010, 2010.

Haywood, A.M., Ridgwell, A., Lunt, D.J., Hill, D.J., Pound, M.J., Dowsett, H.J., Dolan, A.M., Francis, J.E. and Williams, M.: Are there pre-Quaternary geological analogues for a future greenhouse warming?, Philos. T. R. Soc. A, 369, 933-956,

640   https://doi.org/10.1098/rsta.2010.0317, 2011a.

Haywood, A.M., Dowsett, H.J., Robinson, M.M., Stoll, D.K., Dolan, A.M., Lunt, D.J., Otto-Bliesner, B. and Chandler, M.A.: Pliocene Model Intercomparison Project (PlioMIP): experimental design and boundary conditions (Experiment 2), Geosci. Model Dev., 4, 571-577, https://doi.org/10.5194/gmd-4-571-2011, 2011b.

Haywood, A.M., Hill, D.J., Dolan, A.M., Otto-Bliesner, B.L., Bragg, F., Chan, W.L., Chandler, M.A., Contoux, C., Dowsett,

645   H.J., Jost, A., Kamae, Y., Lohmann, G., Lunt, D.J., Abe-Ouchi, A., Pickering, S.J., Ramstein, G., Rosenbloom, N.A., Salzmann, U., Sohl, L., Stepanek, C., Ueda, H., Yan, Q. and Zhang, Z.: Large-scale features of Pliocene climate: results from the Pliocene Model Intercomparison Project, Clim. Past, 9, 191-209, https://doi.org/10.5194/cp-9-191-2013, 2013.

Haywood, A.M., Dowsett, H.J., Dolan, A.M., Rowley, D., Abe-Ouchi, A., Otto-Bliesner, B., Chandler, M.A., Hunter, S.J., Lunt, D.J., Pound, M. and Salzmann, U.: The Pliocene Model Intercomparison Project (PlioMIP) Phase 2: scientific

650   objectives and experimental design, Clim. Past, 12, 663-675, https://doi.org/10.5194/cp-12-663-2016, 2016.

Haywood, A.M., Tindall, J.C., Dowsett, H.J., Dolan, A.M., Foley, K.M., Hunter, S.J., Hill, D.J., Chan, W.-L., Abe-Ouchi, A., Stepanek, C., Lohmann, G., Chandan, D., Peltier, W.R., Tan, N., Contoux, C., Ramstein, G., Li, X., Zhang, Z., Guo, C., Nisancioglu, K.H., Zhang, Q., Li, Q., Kamae, Y., Chandler, M.A., Sohl, L.E., Otto-Bliesner, B.L., Feng, R., Brady, E.C., von der Heydt, A.S., Baatsen, M.L.J. and Lunt, D.J.: The Pliocene Model Intercomparison Project Phase 2: large-scale climate

655   features and climate sensitivity, Clim. Past, 16, 2095-2123, https://doi.org/10.5194/cp-16-2095-2020, 2020.

Heinemann, M., Jungclaus, J. H. and Marotzke, J.: Warm Paleocene/Eocene climate as simulated in ECHAM5/MPI-OM, Clim. Past, 5, 785-802, https://doi.org/10.5194/cp-5-785-2009, 2009.

Hill, D.J., Haywood, A.M., Lunt, D.J., Hunter, S.J., Bragg, F.J., Contoux, C., Stepanek, C., Sohl, L., Rosenbloom, N.A., Chan, W.L., Kamae, Y., Zhang, Z., Abe-Ouchi, A., Chandler, M.A., Jost, A., Lohmann, G., Otto-Bliesner, B.L., Ramstein,

660   G. and Ueda, H.: Evaluating the dominant components of warming in Pliocene climate simulations, Clim. Past, 10, 79-90, https://doi.org/10.5194/cp-10-79-2014, 2014.

Hill, D., Bolton, K. and Haywood, A.: Modelled ocean changes at the Plio-Pleistocene transition driven by Antarctic ice advance, Nat. Commun., 8, 14376, https://doi.org/10.1038/ncomms14376, 2017.

Hunter, S.J., Haywood, A.M., Dolan, A.M. and Tindall, J.C.: The HadCM3 contribution to PlioMIP phase 2, Clim. Past, 15, 1691-1713, https://doi.org/10.5194/cp-15-1691-2019, 2019.

Koenig, S.J., Dolan, A.M., de Boer, B., Stone, E.J., Hill, D.J., DeConto, R.M., Abe-Ouchi, A., Lunt, D.J., Pollard, D., Quiquet, A., Saito, F., Savage, J. and van de Wal, R.: Ice sheet model dependency of the simulated Greenland Ice Sheet in the mid-Pliocene, Clim. Past, 11, 369-381, https://doi.org/10.5194/cp-11-369-2015, 2015.

Levy, R.H., Dolan, A.M., Escutia, C., Gasson, E.G.W., McKay, R.M., Naish, T., Patterson, M.O., Pérez, L.F., Shevenell, A.E., Flierdt, T.v.d., Dickinson, W., Kowalewski, D.E., Meyers, S.R., Ohneiser, C., Sangiorgi, F., Williams, T., Chorley, H.K., Santis, L.D., Florindo, F., Golledge, N.R., Grant, G.R., Halberstadt, A.R.W., Harwood, D.M., Lewis, A.R., Powell, R. and Verret, M.: Antarctic environmental change and ice sheet evolution through the Miocene to Pliocene – a perspective from the Ross Sea and George V to Wilkes Land Coasts, in: Antarctic Climate Evolution (Second Edition), edited by: Florindo, F., Siegert, M., De Santis, L. and Naish, T., Elsevier, 389-521, https://doi.org/10.1016/B978-0-12-819109-5.00014-1, 2022.

Li, X., Guo, C., Zhang, Z., Otterå, O.H. and Zhang, R.: PlioMIP2 simulations with NorESM-L and NorESM1-F, Clim. Past, 16, 183-197, https://doi.org/10.5194/cp-16-183-2020, 2020.

Lee, J.-Y., Marotzke, J., Bala, G., Cao, L., Corti, S., Dunne, J.P., Engelbrecht, F., Fischer, E., Fyfe, J.C., Jones, C., Maycock, A., Mutemi, J., Ndiaye, O., Panickal, S. and Zhou, T.: Future Global Climate: Scenario-Based Projections and Near-Term Information. In Climate Change 2021: The Physical Science Basis. Contribution of Working Group I to the Sixth Assessment Report of the Intergovernmental Panel on Climate Change [Masson-Delmotte, V., Zhai, P., Pirani, A., Connors, S.L., Péan, C., Berger, S., Caud, N., Chen, Y. Goldfarb, L., Gomis, M.I., Huang, M., Leitzell, K., Lonnoy, E., Matthews, J.B.R., Maycock, T.K., Waterfield, T., Yelekçi, O., Yu, R. and Zhou, B. (eds.)]. Cambridge University Press, Cambridge, United Kingdom and New York, NY, USA., 553–672, doi:10.1017/9781009157896.006, 2021.

Lunt, D.J., Haywood, A.M., Schmidt, G.A., Salzmann, U., Valdes, P.J., Dowsett, H.J. and Loptson, C.A.: On the causes of mid-Pliocene warmth and polar amplification, Earth. Planet. Sc. Lett., 321-322, 128-138, https://doi.org/10.1016/j.epsl.2011.12.042, 2012.

Meinshausen, M., Nicholls, Z.R.J., Lewis, J., Gidden, M.J., Vogel, E., Freund, M., Beyerle, U., Gessner, C., Nauels, A., Bauer, N., Canadell, J.G., Daniel, J.S., John, A., Krummel, P.B., Luderer, G., Meinshausen, N., Montzka, S.A., Rayner, P.J., Reimann, S., Smith, S.J., van den Berg, M., Velders, G.J.M., Vollmer, M.K. and Wang, R.H.J.: The shared socio-economic pathway (SSP) greenhouse gas concentrations and their extensions to 2500, Geosci. Model Dev., 13, 3571-3605, https://doi.org/10.5194/gmd-13-3571-2020, 2020.

Myers-Smith, I.H., Kerby, J.T., Phoenix, G.K., Bjerke, J.W., Epstein, H.E., Assmann, J.J., John, C., Andreu-Hayles, L., Angers-Blondin, S., Beck, P.S.A., Berner, L.T., Bhatt, U.S., Bjorkman, A.D., Blok, D., Bryn, A., Christiansen, C.T., Cornelissen, J.H.C., Cunliffe, A.M., Elmendorf, S.C., Forbes, B.C., Goetz, S.J., Hollister, R.D., de Jong, R., Loranty, M.M.,

Macias-Fauria, M., Maseyk, K., Normand, S., Olofsson, J., Parker, T.C., Parmentier, F.-J.W., Post, E., Schaepman-Strub, G., Stordal, F., Sullivan, P.F., Thomas, H.J.D., Tømmervik, H., Treharne, R., Tweedie, C.E., Walker, D.A., Wilmking, M. and Wipf, S.: Complexity revealed in the greening of the Arctic, Nat. Clim. Change, 10, 106-117, https://doi.org/10.1038/s41558-019-0688-1, 2020.

700 Pagani, M., Liu, Z., LaRiviere, J. and Ravelo, A.C.: High Earth-system climate sensitivity determined from Pliocene carbon dioxide concentrations, Nat. Geosci., 3, 27-30, https://doi.org/10.1038/ngeo724, 2010.

Peltier, W.R. and Vettoretti, G.: Dansgaard-Oeschger oscillations predicted in a comprehensive model of glacial climate: A "kicked" salt oscillator in the Atlantic, Geophys. Res. Lett., 41, 7306-7313, https://doi.org/10.1002/2014GL061413, 2014.

Salzmann, U., Haywood, A. M., Lunt, D. J., Valdes, P. J. and Hill, D. J.: A new global biome reconstruction and data-model

705 comparison for the Middle Pliocene, Global Ecol. Biogeogr., 8, 432-447, https://doi.org/10.1111/j.1466-8238.2008.00381.x, 2008.

Seki, O., Foster, G.L., Schmidt, D.N., Mackensen, A., Kawamura, K. and Pancost, R.D.: Alkenone and boron-based Pliocene pCO$_2$ records, Earth Planet. Sc. Lett., 292, 201-211, https://doi.org/10.1016/j.epsl.2010.01.037, 2010.

Sherwood, S.C., Webb, M.J., Annan, J.D., Armour, K.C., Forster, P.M., Hargreaves, J.C., Hegerl, G., Klein, S.A., Marvel,

710 K.D., Rohling, E.J., Watanabe, M., Andrews, T., Braconnot, P., Bretherton, C.S., Foster, G.L., Hausfather, Z., von der Heydt, A.S., Knutti, R., Mauritsen, T., Norris, J.R., Proistosescu, C., Rugenstein, M., Schmidt, G.A., Tokarska, K.B., and Zelinka, M.D: An Assessment of Earth's Climate Sensitivity Using Multiple Lines of Evidence, Rev. Geophys., 58, e2019RG000678, https://doi.org/10.1029/2019RG000678, 2020.

Stepanek, C., Samakinwa, E., Knorr, G., and Lohmann, G.: Contribution of the coupled atmosphere–ocean–sea ice–

715 vegetation model COSMOS to the PlioMIP2, Clim. Past, 16, 2275-2323, https://doi.org/10.5194/cp-16-2275-2020, 2020.

Sun, Y., Ramstein, G., Contoux, C. and Zhou, T.: A comparative study of large-scale atmospheric circulation in the context of a future scenario (RCP4.5) and past warmth (mid-Pliocene), Clim. Past, 9, 1613-1627, https://doi.org/10.5194/cp-9-1613-2013, 2013.

Tan, N., Contoux, C., Ramstein, G., Sun, Y., Dumas, C., Sepulchre, P. and Guo, Z.: Modeling a modern-like pCO$_2$ warm

720 period (Marine Isotope Stage KM5c) with two versions of an Institut Pierre Simon Laplace atmosphere–ocean coupled general circulation model, Clim. Past, 16, 1-16, https://doi.org/10.5194/cp-16-1-2020, 2020.

Williams, C.J.R., Sellar, A.A., Ren, X., Haywood, A.M., Hopcroft, P., Hunter, S.J., Roberts, W.H.G., Smith, R.S., Stone, E.J., Tindall, J.C. and Lunt, D.J.: Simulation of the mid-Pliocene Warm Period using HadGEM3: experimental design and results from model-model and model-data comparison, Clim. Past, 17, 2139-2163, https://doi.org/10.5194/cp-17-2139-2021,

725 2021.

Yang, S.-K. and Smith, G.L.: Further Study on Atmospheric Lapse Rate Regimes, J. Atmos. Sci., 42, 961-966, 1985.